Characterization of biaxial orientation in poly(ethylene terephthalate) by means of refractive index measurements and Raman and infra-red spectroscopies

D. A. Jarvis†, I. J. Hutchinson*, D. I. Bower and I. M. Ward
Department of Physics, The University of Leeds, Leeds LS2 9JT, UK
(Received 27 April 1979)

The three principal refractive indices of a film of poly(ethylene terephthalate), prepared by drawing an amorphous melt-extruded sheet at constant width between rollers whose speeds were set to give a nominal draw ratio of 3.5:1, were found to be 1.645, 1.573 and 1.541. Thirty-six measurements of the scattered intensity for the 1616 cm^{-1} Raman line were made for various combinations of orientations of the electric vectors of the incident and scattered light with respect to the sample and six absorbances were determined for each of the 1017 and 875 cm^{-1} infra-red peaks with the polarization vector of the radiation in different orientations with respect to the sample. From the Raman measurements five parameters P^r_{200}, P^r_{220}, P^r_{400}, P^r_{420}, and P^r_{440} which characterize the distribution of orientations of the benzene rings were deduced. Values of P^r_{200} and P^r_{220}, in good agreement with the Raman values, were also deduced from the infra-red measurements, and a further two parameters, P^r_{202} and P^r_{222} were deduced from infra-red and Raman results combined. The four quantities P^r_{200}, P^r_{220}, P^r_{202} and P^r_{222} are shown to be consistent with the refractive index measurements using either of two alternative models for the chain conformation. The results indicate that there is slight preferential orientation of the chain axes *out* of the plane of the film, an unexpected result, but that there is also some preferential orientation of the planes of the benzene rings *towards* the plane of the film, in agreement with earlier X-ray measurements on similar films.

INTRODUCTION

Several techniques are used for the characterization of molecular orientation in polymers of low crystallinity. Among the more important of these are broad-line n.m.r.[1,2], polarized fluorescence[3,4], Raman[5–7] and infra-red[8] spectroscopies, and all these methods have been applied successfully to uniaxially-drawn polymers. Although the extension to biaxially oriented films was attempted by n.m.r.[1], it was clear that this technique possesses severe limitations, including the necessity to have a precise knowledge of any changes in molecular conformation which take place during drawing. The fluorescence method usually requires either the modification of the polymer chains to make them fluorescent or the addition to the polymer of fluorescent probe molecules, so that this method gives information somewhat indirectly about orientation of ordinary polymer chains. It thus appears that the most complete characterization of biaxially-drawn systems of low crystallinity requires measurements by vibrational spectroscopy.

In principle, Raman spectroscopy can provide more information than infra-red spectroscopy about molecular orientation, but infra-red data may be used as a check on and supplement to the Raman data and may sometimes more readily give information about conformational changes. These two techniques have therefore been developed to study changes in molecular orientation and conformation in a system which is of both fundamental and technological interest, biaxially-oriented poly(ethylene terephthalate) (PET) sheet. The present paper is, however, concerned only with molecular orientation.

Before the experimental work is considered, the theoretical aspects of the study of orientation by infra-red and Raman spectroscopy will be discussed, with emphasis on the application to polymer systems with biaxial symmetry. The measurement of refractive indices can provide useful additional information about molecular orientation, and the theory of the relationship between the refractive indices and the molecular orientation for biaxial symmetry will also be considered.

THEORY

Orientation distribution functions

It will be assumed for the purposes of discussing the refractive indices, the infra-red absorption or the Raman scattering, that the oriented polymer may be considered to be composed of non-interacting, anisotropic structural units. The nature of the effective structural units depends upon which technique is used in investigating the polymer. If a coordinate system is defined in each of the structural units, the orientation of a particular unit with respect to a coordinate system fixed in the sample may be described by the Euler angles θ, ϕ and ψ. These are shown in *Figure 1*, where

* Present address: ICI Corporate Laboratory, Runcorn, Cheshire, UK
† Present address: H. H. Wills Physics Laboratory, University of Bristol, UK

0032–3861/80/010041–14$02.00

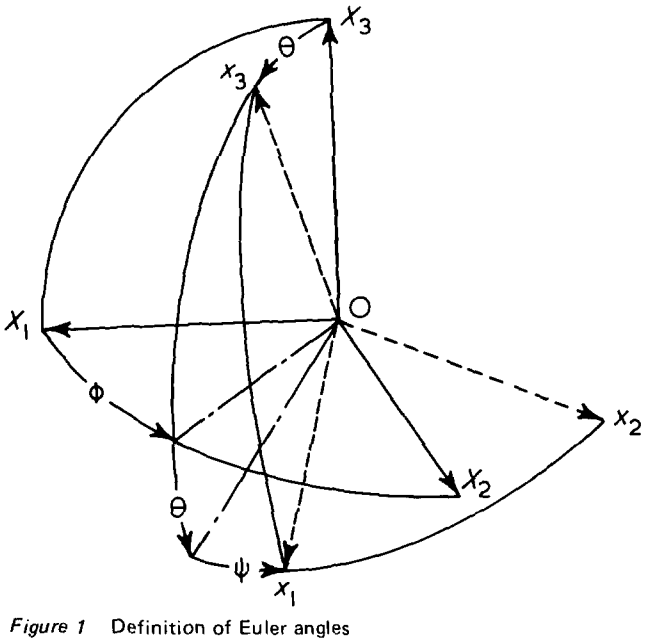

Figure 1 Definition of Euler angles

the $OX_1X_2X_3$ system of axes is fixed in the sample and the $Ox_1x_2x_3$ system is fixed in the structural unit. The angles θ and ϕ are the polar and azimuthal angles, respectively, of the Ox_3 axis with respect to the $OX_1X_2X_3$ system, and the angle ψ represents a rotation about the Ox_3 axis which takes the Ox_1 axis out of the x_3OX_3 plane.

It is usual to choose the axes of the fixed coordinate system to be coincident with the symmetry axes of the polymer sample and the axes of each of the other coordinate systems to be coincident with the symmetry axes (if there are any) of the corresponding structural unit. It will be assumed in the present discussion that the polymer sample has at least the symmetry of the orthorhombic point group D_2, i.e. that it has three mutually perpendicular two-fold axes of rotation; strictly speaking, this is the symmetry of the function which describes the distribution of orientations of the structural units. In addition, it will be assumed that each type of structural unit considered has at least the symmetry of point group D_2 with respect to the axes $Ox_1x_2x_3$ or if it does not, that it behaves during the production of orientation as if it does have at least this symmetry. This means that the distribution is assumed to remain unchanged if any structural unit is rotated through 180°C about its Ox_1, Ox_2 or Ox_3 axis.

A function describing the distribution of orientations of the structural units may be written in terms of the three Euler angles. It is convenient to expand this distribution function in a series of generalized spherical harmonics, i.e.:

$$N(\theta,\phi,\psi) = \sum_{l=0}^{\infty} \sum_{m=-l}^{+l} \sum_{n=-l}^{+l} P_{lmn} Z_{lmn}(\cos\theta) e^{-im\phi} e^{-in\psi} \quad (1)$$

$N(\theta,\phi,\psi)\sin\theta d\theta d\phi d\psi$ is equal to the fraction of units whose axes lie in the generalized solid angle $\sin\theta d\theta d\phi d\psi$ and the Z_{lmn} are a generalization of the Legendre functions. Because the functions $Z_{lmn}(\cos\theta)e^{-im\phi}e^{-in\psi}$ are mutually orthogonal, the coefficients, P_{lmn}, of this series are averages of functions $p_{lmn}(\theta,\phi,\psi)$ taken over the structural units in the sample. These functions are the same as $Z_{lmn}(\cos\theta)e^{im\phi}e^{in\psi}$ apart from constant factors, and when $m \neq 0$ and/or $n \neq 0$ they are complex. The assumption of at least the symmetry of point group D_2 for both the material and the structural units means that the P_{lmn} are only non-zero if m and n are even[9]. Infra-red spectroscopy and measurements of refractive indices can give information about P_{lmn} only for $l = 2$ and Raman spectroscopy only for $l = 2$ or 4. For a real distribution these restrictions on l, m and n ensure that P_{lmn} is real and that:

$$P_{lmn} = P_{l\bar{m}n} = P_{lm\bar{n}} = P_{l\bar{m}\bar{n}} \quad (2)$$

Nevertheless, the summation in equation (1) will continue to be taken formally over positive and negative values of m and n.

In this paper a non-normalized form of the Z_{lmn} is chosen which makes $P_{000} = 1$ and makes P_{l00} equal to the average over the distribution of the lth order Legendre polynomial in $\cos\theta$. The coefficients ν_{lmn} which replace the P_{lmn} if Z_{lmn} is normalized so that:

$$\int_0^{\pi} [Z_{lmn}(\cos\theta)]^2 \sin\theta d\theta = 1$$

as it is in reference[9], are given by:

$$P_{lmn} = \frac{4\pi^2}{N_{lmn}} \nu_{lmn} \quad (3)$$

where

$$N^2_{lmn} = N^2_{l\bar{m}n} = N^2_{lm\bar{n}} = N^2_{l\bar{m}\bar{n}} = \frac{2l+1}{2} \frac{(l+m)!(l-n)!}{(l-m)!(l+n)!} \frac{1}{[(m-n)!]^2}$$

for $m > n$ (4a)

and

$$N^2_{lmn} = N^2_{lnm} \text{ for } m < n \quad (4b)$$

For m, $n \neq 0$, the present set of coefficients is slightly different from the set chosen by Nomura *et al.*[10].

There are four important combinations of sample symmetry and symmetry of the structural units which define simpler forms of overall symmetry than that already considered and these will now be discussed, starting with the simplest.

(i) Uniaxial symmetry of the distribution function about the OX_3 *axis and no preferred orientation of the structural units about their* Ox_3 *axes.* Both ϕ and ψ take random values and the P_{lmn} are only non-zero for $m = n = 0$, giving the set of coefficients $P_{l00} = \langle p_{l00}(\theta)\rangle$, where the brackets $\langle\rangle$ denote an average over the structural units in the sample.

The first few coefficients are:

$$P_{000} = 1 \quad (5a)$$

$$P_{200} = \frac{1}{2}\langle 3\cos^2\theta - 1\rangle \quad (5b)$$

$$P_{400} = \frac{1}{8}\langle 3 - 30\cos^2\theta + 35\cos^4\theta\rangle \quad (5c)$$

These coefficients are those with which previous work on uniaxial materials has mainly been concerned.

(ii) Biaxial symmetry of the distribution function and no preferred orientation of the structural units about their Ox_3 *axes.* ψ, but not ϕ, takes random values and this means that the P_{lmn} are non-zero only for $n = 0$. For $m = 0$ the coefficients are as given above, and for $m \neq 0$ the first few coefficients reduce to:

$$P_{220} = \frac{1}{4}\langle(1 - \cos^2\theta)\cos 2\phi\rangle \quad (6a)$$

$$P_{420} = \frac{1}{24}\langle(-1 + 8\cos^2\theta - 7\cos^4\theta)\cos 2\phi\rangle \quad (6b)$$

$$P_{440} = \frac{1}{16}\langle(1 - 2\cos^2\theta + \cos^4\theta)\cos 4\phi\rangle \quad (6c)$$

(iii) General uniaxial statistical symmetry. In this case ϕ, but not necessarily ψ, takes random values, which means that the P_{lmn} are non-zero only for $m = 0$. For $n = 0$ the coefficients are as given above and for $n \neq 0$ the first few coefficients reduce to:

$$P_{202} = \frac{1}{4}\langle(1 - \cos^2\theta)\cos 2\psi\rangle \quad (7a)$$

$$P_{402} = \frac{1}{24}\langle(-1 + 8\cos^2\theta - 7\cos^4\theta)\cos 2\psi\rangle \quad (7b)$$

$$P_{404} = \frac{1}{16}\langle(1 - 2\cos^2\theta + \cos^4\theta)\cos^4\psi\rangle \quad (7c)$$

(iv) General biaxial statistical symmetry. None of the Euler angles may be assumed to take random values and the P_{lmn} may be non-zero for all even values of m and n. If $m = 0$ and/or $n = 0$ the sets of coefficients are as given above and when both m and n are non-zero the first few P_{lmn} reduce to:

$$P_{222} = \frac{1}{4}\langle(1 + \cos^2\theta)\cos 2\phi\cos 2\psi - 2\cos\theta\sin 2\phi\sin 2\psi\rangle \quad (8a)$$

$$P_{422} = \frac{1}{4}\langle(1 - 6\cos^2\theta + 7\cos^4\theta)\cos 2\phi\cos 2\psi + (5\cos\theta - 7\cos^3\theta)\sin 2\phi\sin 2\psi\rangle \quad (8b)$$

$$P_{442} = \frac{1}{16}\langle(1 - \cos^4\theta)\cos 4\phi\cos 2\psi - 2(\cos\theta - \cos^3\theta)\sin 4\phi\sin 2\psi\rangle \quad (8c)$$

$$P_{424} = \frac{1}{16}\langle(1 - \cos^4\theta)\cos 2\phi\cos 4\psi - 2(\cos\theta - \cos^3\theta)\sin 2\phi\sin 4\psi\rangle \quad (8d)$$

$$P_{444} = \frac{1}{16}\langle(1 + 6\cos^2\theta + \cos^4\theta)\cos 4\phi\cos 4\psi - 4(\cos\theta + \cos^3\theta)\sin 4\phi\sin 4\psi\rangle \quad (8e)$$

The complete set of coefficients P_{lmn} described above provides a fairly detailed characterization of the distribution of orientations of the structural units within a material, and this work is concerned with the measurement and interpretation of seven of them.

Relationship between the P_{lmn} *and the refractive indices*

It is possible to obtain a relationship between the P_{lmn} and the refractive indices, provided that the components of the polarizability tensor for the structural unit are known and it is assumed that the polarizabilities of all structural units in unit volume may be added to give the volume polarizability of the sample. For a uniaxially-drawn polymer with no preferred orientation of the structural units about their Ox_3 axes, Cunningham *et al.*[11] showed that the two principal refractive indices, n_3 and n_1 (=n_2), depend on the value of P_{200} and the principal electronic polarizabilities of the structural unit in the following way:

$$\frac{\phi_3^e - \phi_1^e}{\phi_3^e + 2\phi_1^e} = \frac{\Delta\alpha^e}{3\alpha_0^e}P_{200} \quad (9)$$

where

$$\phi_i^e = \frac{4\pi}{3}N^e\langle\alpha_i^e\rangle = \frac{n_i^2 - 1}{n_i^2 + 2} \quad (10)$$

$$\alpha_0^e = \frac{1}{3}(\alpha_1^e + \alpha_2^e + \alpha_3^e) \quad (11)$$

and

$$\Delta\alpha^e = \alpha_3^e - \frac{\alpha_1^e + \alpha_2^e}{2} \quad (12)$$

N^e is the number of structural units in unit volume and α_1^e, α_2^e and α_3^e are the principal components of the electronic polarizability tensor for a unit. It was assumed that one of the principal axes of the polarizability tensor, corresponding to α_3^e, was parallel to Ox_3.

For a polymer with the general type of biaxial distribution discussed in (iv) above, the relationship between the refractive indices and the polarizability tensor is more complicated. It is first necessary to realize that the principal axes of the polarizability tensor may not coincide with a particular set of axes $Ox_1x_2x_3$ chosen within the structural unit. This will be discussed in detail in a later section when two different models for the structure of the molecular chain in amorphous PET are considered. Nevertheless, because the structural units are assumed in the present work to behave during orientation as if they have the symmetry of point group D_2 with respect to $Ox_1x_2x_3$, an effective polarizability tensor can be defined which is the mean of the actual tensor and the three different but related tensors which may be obtained by rotating it through 180° about the axes Ox_1, Ox_2 or Ox_3. This effective tensor has $Ox_1x_2x_3$ as its principal axes and the corresponding principal components, α_1^e, α_2^e and α_3^e, are the components α_{11}^e, α_{22}^e and

α^e_{33}, respectively, of the true polarizability tensor expressed with respect to $Ox_1x_2x_3$.

It may then be shown that the equations corresponding to equation (9) are:

$$\frac{2\phi^e_3 - \phi^e_1 - \phi^e_2}{\phi^e_1 + \phi^e_2 + \phi^e_3} = \frac{2\Delta\alpha^e}{3\alpha^e_0} P_{200} + \frac{2\delta\alpha^e}{\alpha^e_0} P_{202} \quad (13a)$$

$$\frac{\phi^e_1 - \phi^e_2}{\phi^e_1 + \phi^e_2 + \phi^e_3} = \frac{4\Delta\alpha^e}{3\alpha^e_0} P_{220} + \frac{2\delta\alpha^e}{3\alpha^e_0} P_{222} \quad (13b)$$

where

$$\delta\alpha^e = \alpha^e_1 - \alpha^e_2 \quad (14)$$

and the remaining symbols have the same significance as in equations (10) to (12). Kashiwagi *et al.*[1] have previously considered the relationship between the refractive indices and the molecular polarizabilities for a biaxially-oriented polymer [(ii) above], but they do not quote the general result expressed in equations (13).

Raman scattering

The Raman effect may be used for determining the P_{lmn} for l = 2 and 4 and it has already been used for studying orientation in uniaxially drawn polymers[5–7]. The relationship between the P_{lmn} and the experimentally observed scattered intensities has been discussed in detail by Bower[12,13] and only a brief summary will now be presented.

For a polymer with a birefringence as great as that of PET it is not possible to obtain useful information from intensity measurements for even relatively low degrees of molecular orientation, unless the polarization directions of the incident and scattered light are each parallel to one of the axes OX_1, OX_2 or OX_3. If the polarization directions of the incident light and the analyser are parallel to the axes OX_j and OX_i, respectively, the intensity of the scattered radiation, I_{ij}, for a particular mode of vibration, is given by

$$I_{ij} = I_0 \sum \alpha^2_{ij} \quad (15)$$

The quantities α_{ij} are the components of the Raman tensor for the vibration studied expressed with respect to the axes $OX_1X_2X_3$, I_0 is a constant depending on the incident light intensity and instrumental factors, and the summation is over all scattering units contributing to the observed intensity.

The scattered intensity is therefore determined, apart from a constant factor, by the quantities $\langle\alpha^2_{ij}\rangle$. These quantities depend on the principal components α_1, α_2 and α_3 of the Raman tensor and on the distribution of orientations of the principal axes of the Raman tensors. They may be written as:

$$\langle\alpha^2_{ij}\rangle = \sum_{lmn} P_{lmn} A^{ij}_{lmn} \quad (16)$$

provided that the axes $Ox_1x_2x_3$ are chosen to coincide with the principal axes of the Raman tensor. The A^{ij}_{lmn} are second-order functions of α_1, α_2 and α_3 and differ from the corresponding A^{ijij}_{lmn} given by Bower[12] only by a factor of N_{lmn}. Equations (15) and (16) lead to:

$$I_{ij} = I_0 N_0 \sum_{lmn} P_{lmn} A^{ij}_{lmn} \quad (17)$$

where N_0 is the number of effective scatterers, so that each of the six intensities I_{ij} is related linearly to the quantities P_{lmn}.

The present work is concerned with measurements of the intensity of Raman scattering from the 1616 cm^{-1} line in PET, which have previously been shown to provide useful information about molecular orientation. This line corresponds to an almost pure benzene ring vibration[14,15], the approximate form of which is shown in *Figure 2*, so that the structural unit for which the P_{lmn} are most directly determined is the benzene ring, and these values will be written P^r_{lmn}. The principal axes of the Raman tensor for this vibration coincide with the ring axes $Ox^r_1x^r_2x^r_3$ shown in *Figure 2*. For this choice of Ox^r_3, previous work[5,7] has shown that $\alpha_1 = \alpha_2$, to a good approximation, and has provided a value for the ratio $r = \alpha_1/\alpha_3$. For such a 'cylindrical' tensor $A^{ij}_{lmn} = 0$ unless n = 0, since rotation of such a tensor about its symmetry axis can clearly have no effect on the scattered intensity. Since $P^r_{000} = 1$, equations (17) become:

$$I'_{11} = A + B(P^r_{200} - 6P^r_{220}) + C(3P^r_{400} - 60P^r_{420} + 70P^r_{440}) \quad (18a)$$

$$I'_{22} = A + B(P^r_{200} + 6P^r_{220}) + C(3P^r_{400} + 60P^r_{420} + 70P^r_{440}) \quad (18b)$$

$$I'_{33} = A - 2BP^r_{200} + 8CP^r_{400} \quad (18c)$$

$$I'_{23} = D - E(P^r_{200} - 6P^r_{220}) - 4C(P^r_{400} + 15P^r_{420}) \quad (18d)$$

$$I'_{31} = D - E(P^r_{200} + 6P^r_{220}) - 4C(P^r_{400} - 15P^r_{420}) \quad (18e)$$

$$I'_{12} = D + 2EP^r_{200} + C(P^r_{400} - 70P^r_{440}) \quad (18f)$$

where

$$I'_{ij} = I_{ij}/(\alpha^2_3 I_0 N_0) \quad (19)$$

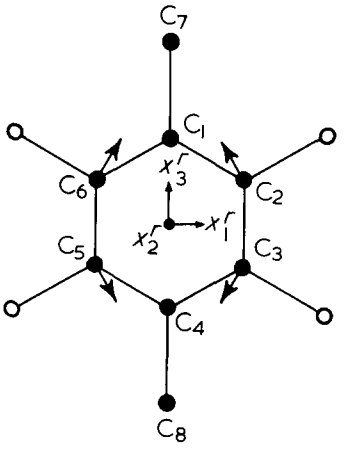

Figure 2 Approximate form of vibration assigned to 1616 cm^{-1} Raman line. Also shown are the 'ring axes' $Ox^r_1x^r_2x^r_3$

and

$$A = (8r^2 + 4r + 3)/15 \quad (20a)$$

$$B = (8r^2 - 2r - 6)/21 \quad (20b)$$

$$C = (8r^2 - 16r + 8)/280 \quad (20c)$$

$$D = (r^2 - 2r + 1)/15 \quad (20d)$$

$$E = (-2r^2 + 4r - 2)/42 \quad (20e)$$

If the value of r is known, equations (18) are six linear simultaneous equations in the six quantities $(\alpha_3^2 I_0 N_0)^{-1}$, P^r_{200}, P^r_{220}, P^r_{400} and P^r_{420} and P^r_{440}.

Infra-red absorption

The theory involved in the determination of P_{200} for a uniaxially-drawn polymer from measurements of infra-red absorption has previously been given by Cunningham *et al.*[11]. By assuming that the angle, θ_m, between the chain axis direction and the transition moment vector, $\vec{\mu}$, for the vibrational mode considered was constant, and that there was no preferred orientation of the transition moment vector around the chain axis, they obtained the following expression for P^c_{200}, which refers to the orientation of the chains when the chain-axis is chosen as Ox_3:

$$\frac{\phi_3 - \phi_1}{\phi_3 + 2\phi_1} = p_{200}(\theta_m)P^c_{200} \quad (21)$$

where

$$\phi_i = \frac{4\pi}{3} N\langle\alpha_i''\rangle = 6n_i k_i\{(n_i^2 + 2)^2 + (2n_i^2 - 4)k_i^2 + k_i^4\}^{-1} \quad (22)$$

The quantities n_i and k_i are the real and imaginary parts, respectively, of the complex principal refractive indices $\hat{n}_i = n_i - ik_i$ for the particular infra-red-active vibration under consideration ($n_1 = n_2$, $k_1 = k_2$ for uniaxial orientation), N is the concentration of absorbing species per unit volume, and the quantities $\langle\alpha_i''\rangle$ are the imaginary parts of the principal average complex polarizabilities. The values of k_i may be calculated from the experimentally observed absorbances. This theory has been applied to the study of orientation in PET film by Cunningham *et al.*[8].

When considering a biaxially-drawn polymer and dropping the assumption of no preferred orientation around Ox_3 it is useful to choose the $Ox_1x_2x_3$ coordinate system so that the Ox_3 axis is coincident with some significant direction in the polymer chain and the transition moment vector lies in the Ox_2x_3 plane. In the present work it is convenient to choose $Ox_1x_2x_3$ to coincide with the set of axes $Ox^r_1x^r_2x^r_3$ already defined in the benzene ring, since the information to be obtained from the present measurements of infra-red spectra also refers directly to the benzene rings. By means of a calculation similar to that of Cunningham *et al.*[11] the following two relationships corresponding to equation (21) may be obtained:

$$\frac{2\phi_3 - \phi_1 - \phi_2}{\phi_1 + \phi_2 + \phi_3} = 2p_{200}(\theta_m)P^r_{200} + 4p_{200}(\theta_m)P^r_{202} - 4P^r_{202} \quad (23a)$$

$$\frac{\phi_1 - \phi_2}{\phi_1 + \phi_2 + \phi_3} = 4p_{200}(\theta_m)P^r_{220} + \frac{4}{3}p_{200}(\theta_m)P^r_{222} - \frac{4}{3}P^r_{222} \quad (23b)$$

In these equations θ_m has been redefined to be the angle between the transition moment and the Ox^r_3 axis (which coincides with the C_1–C_4 direction in the benzene ring).

For PET there are two infra-red absorption peaks associated with benzene ring vibrations for which the directions of the transition moment vectors are well known[16,17]. These are the 1017 and 875 cm^{-1} absorptions (see *Figure 3*). The vibration giving rise to the peak at 1017 cm^{-1} has its transition moment vector along the C_1–C_4 direction, Ox^r_3. Thus, infra-red absorption measurements on this peak combined with equations (23) with $\theta_m = 0$, i.e. $p_{200}(\theta_m) = 1$, give values of P^r_{200} and P^r_{220} which should agree with those obtained from Raman scattering measurements on the 1616 cm^{-1} line. The vibration giving rise to the peak at 875 cm^{-1} has its transition moment vector normal to the plane of the benzene ring. The infra-red absorption measurements on this peak, combined with equations (23) with $\theta_m = 90°$, i.e. $p_{200}(\theta_m) = -\frac{1}{2}$, thus give values of the quantities $(P^r_{200} + 6P^r_{202})$ and $(P^r_{220} + P^r_{222})$ and it is thus possible to obtain P^r_{202} and P^r_{222} by combining these results with those from measurements on the peak at 1017 cm^{-1} or from Raman measurements on the 1616 cm^{-1} line.

Equations (23) and (22) show that in order to determine the orientation parameters P_{2mn} by means of infra-red spectroscopy it is necessary to determine the values of the six quantities n_i and k_i at the wavelength of the particular peaks of absorbance involved. As shown in the Appendix, this can be done by making six measurements of absorption for each peak. In two 'normal-film' measurements, the radiation propagates in the direction normal to the plane of the film and the polarization direction is parallel or perpendicular to the draw direction. In one pair of 'tilted-film' measurements the radiation propagates in the plane containing the draw direction and the normal to the film and is polarized either in this plane or perpendicular to it, i.e. the film is 'tilted' by rotating through a fixed angle (usually 45°) about an axis lying in the film and normal to the draw direction. In the second pair of 'tilted-film' measurements the radiation propagates in the plane containing this latter axis and the normal to the film and is polarized either in this plane or parallel to the draw direction, i.e. the film is 'tilted' about the draw direction.

The theory shows that for the normal-film experiment the absorption depends simply on the appropriate value of k_i, whereas for the tilted-film experiments it depends in a more complicated way on either one or two pairs of values of n_i and k_i. In a completely correct analysis the six sets of absorption data would be used to calculate the three values of n_i and the three values of k_i for all points in the spectrum in the region of the absorption peaks considered. Unless k_i is large, equation (22) reduces, to a good approximation, to:

$$\phi_i = \frac{4\pi}{3} N\langle\alpha_i''\rangle = 6n_i k_i/(n_i^2 + 2)^2 \quad (24)$$

and the spectrum of the quantity $n_i k_i/(n_i^2 + 2)^2$ against frequency should then be a sum of Lorentzian peaks, one due to each absorption. By analysing this spectrum into a set of overlapping Lorentzians the value of ϕ_i can thus be found for each absorption. If, however, the absorption peaks are

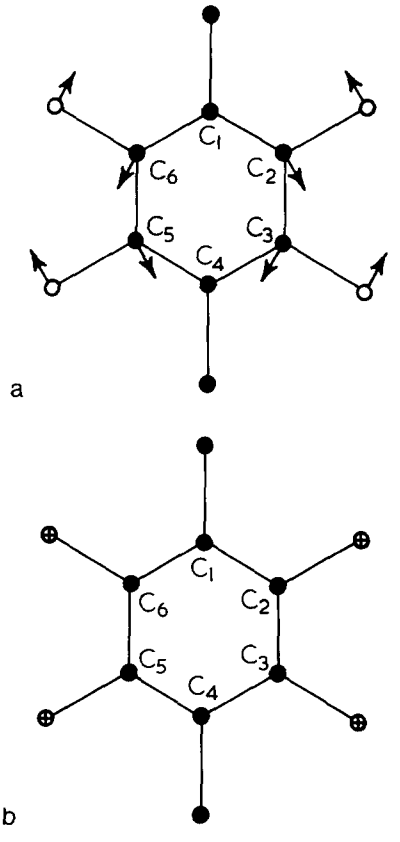

Figure 3 Approximate forms of the vibrations assigned to the infrared absorption peaks at (a) 1017 cm^{-1}; (b) 875 cm^{-1}

narrow and the absorption is not too great it may be shown (see Appendix) that it is a good approximation to treat the directly observed absorbance spectrum as the sum of a set of overlapping Lorentzians, the peak heights of which are related to n_i and k_i.

EXPERIMENTAL DETAILS AND PRIMARY DATA

Materials

The measurements were undertaken on one-way drawn PET film of thickness 28.7 μm, obtained from Imperial Chemical Industries Limited, Plastics Division, Welwyn Garden City. The film had been prepared by drawing the amorphous melt-extruded sheet of PET at constant width between moving rollers. The ratio of the speed of the feed roll to that of the draw roll was set to give a nominal draw ratio of 3.5:1. Measurements of the three principal refractive indices showed that the resulting film was biaxial, as would be expected. In the remainder of the paper, we choose the axes $OX_1X_2X_3$ so that OX_3 is parallel to the draw direction and OX_1 lies in the plane of the film.

Refractive index measurements

An Abbé refractometer was used to measure the three principal refractive indices of the film at the wavelength of the sodium D lines. They were found to be

$n_1 = 1.573$

$n_2 = 1.541$

$n_3 = 1.645$

The uncertainty of each of these values is ±0.001.

Raman measurements

The apparatus used to record the Raman spectra has been described previously[6]. It consists essentially of a CRL model 52A Ar^+ laser, of which the 488 nm line is used to excite the spectra, and a Coderg PHO double monochromator to analyse the spectra. The signal from the monochromator was detected by a photomultiplier tube whose signal/noise ratio was increased by cooling to −30°C and by application of an axial magnetic field. The resultant output was amplified by a low-noise d.c. amplifier and recorded on a chart recorder.

Nine simple scattering configurations may be considered, i.e. the incident light may enter along any one of the three principal axes of symmetry of the sample and the scattered light may be observed in two directions at 90° and one at 180° to the incident light. For each of these configurations there are four combinations of polarization directions for the polarizer and analyser, giving a total of 36 intensities which may be observed. All 36 scattered intensities for the 1616 cm^{-1} line were measured for the sample. As already mentioned, for a material which has biaxial symmetry only, six of these intensities are independent. When the sample was positioned with the plane of the film normal to the incident beam the beam was focussed near but not on the sample. For the other sample configurations the incident beam was focussed onto the edge of the sample and the laser power was reduced so as not to damage the sample. In order to minimize polarization scrambling the sample was cut and clamped in a holder so that for each of the configurations for which the direction of propagation of the incident or scattered light was in the plane of the film the maximum distance the beam travelled in the sample was 1 mm.

The 1616 cm^{-1} line in the Raman spectrum of PET occurs in a region well clear of other lines, and its intensity was therefore read directly from the chart record as peak height above an estimated background (which was a straight line in the region of the 1616 cm^{-1} line). The intensities were corrected for the small differential polarization sensitivity of the spectrometer and the inequality of the intensities of the exciting radiation for the two incident polarizations, which was significant only for the 180° scattering configurations.

The nine sets of four intensity measurements obtained for each sample configuration were scaled to a common value of N_0I_0 in the following way. If the required scaling factors associated with the nine sets are q_1 to q_9, the mean values of the six independent Raman intensities may be written in terms of the q_i, and thus the sum of the squares of the deviations of the measured intensities from their mean values, ΣD^2, may also be written in terms of these quantities. The q_i were chosen so as to minimize the value of ΣD^2, subject to the condition that the mean of the scaled values of I_{33} was equal to 100. (I_{33} is the largest intensity for the 1616 cm^{-1} line). The resulting scaled intensities and the mean values of the six independent Raman intensities are shown in *Table 1*. X_1X_1 represents a 180° scattering configuration with light incident along the OX_1 axis; X_1X_2 represents a 90° scattering configuration with light incident in the OX_1 direction and the Raman scattered light detected in the OX_2 direction, etc. The Table shows that the data is highly self-consistent. In particular, there is good agreement between the values of I_{ij} and I_{ji} for $i \neq j$ and in subsequent analysis the means of these values will be used and they will be called $\bar{I}_{ij}$. A second set of 36 measurements was made on a second sample from the film and was analysed in the same

Table 1 Raman intensities 1616 cm^{-1} line

Scatter geometry	I_{11}	I_{22}	I_{33}	I_{12}	I_{21}	I_{13}	I_{31}	I_{23}	I_{32}
X_1X_1		37.5	95.7					37.2	35.2
X_1X_2			99.8	24.1		23.8			35.9
X_1X_3		31.1		24.1		27.9		33.6	
X_2X_1			103.1		21.3		22.0	27.3	
X_2X_2	25.7		101.3			23.5	21.9		
X_2X_3	27.2				22.4	25.3		33.4	
X_3X_1		33.4			28.5		23.0		26.8
X_3X_2	24.5			29.4			24.8		27.4
X_3X_3	26.3	29.2		26.9	27.6				
Mean	25.9	32.8	100.0	26.2	25.0	25.1	22.9	32.9	31.3
R.m.s. deviation	1.0	3.1	2.7	2.2	3.1	1.7	1.2	3.6	4.2
Mean				25.5		24.0		32.1	
R.m.s. deviation				2.8		1.9		4.0	

way. The values of I_{ii} and I_{ij} obtained agreed with the first set within the uncertainties shown in *Table 1*.

Infra-red measurements

The infra-red measurements were made using a modified Perkin–Elmer 157 spectrometer equipped with a wire-grid polarizer in the common beam.

The normal-film experiments were performed with the sample sandwiched between potassium bromide plates and the tilted-film experiments were performed with the sample sandwiched between 45° prisms of potassium bromide. The angle of tilt was thus 45°. In each case layers of nujol were used to provide optical matching. The attenuator in the reference beam was adjusted for each spectrum so as to get as much as possible of the required region of the spectrum lying between 10 and 90% transmission. Recording was by chart recorder as transmission against wavenumber. The transmission was read off at equal wavenumber intervals and transferred to punched tape for processing.

The first step in processing was to convert the transmission spectra into absorbance spectra, defining the apparent absorbance A as $\log_{10}(I/I_0)$ where I and I_0 are the transmitted and incident intensities, respectively. Each spectrum was then analysed into a set of overlapping Lorentzian peaks and a linear background. The number of peaks used was the minimum required to obtain a good fit to the spectrum and second derivative spectra were used as a guide to required peaks. The procedure used was to fit the two 'normal film' spectra allowing the positions and half-intensity widths of the peaks to vary freely and then to fit both the normal-film and tilted-film spectra keeping the positions and half-intensity widths fixed at the values found from the fits to the normal-film spectra.

In each of the regions near 875 and 1017 cm^{-1} it was necessary to use two Lorentzians to obtain a good fit. In some of the spectra obtained in a related investigation[18], where a wide range of PET samples of different structures were examined, the two peaks in the 1017 cm^{-1} region were clearly resolved. However, it was never possible to resolve the peaks near 875 cm^{-1}. It may be that there is actually only one asymmetric peak in this region and the 875 cm^{-1} i.r. absorption has been used to characterize molecular orientation in uniaxially-oriented PET sheets with considerable success[8], on the basis of the direct measurement of peak intensities.

Unfortunately the sample was rather too thick to obtain very accurate values of the absorbances for the 1017 cm^{-1} peaks, since the transmitted intensity was too low to be measured accurately over the central region of the peak and the fitting had to be restricted to the wings of these lines (see *Figure 4*). The peak absorbances calculated from the fits are shown in *Table 2*, together with the full widths of the peaks at half the maximum absorbance.

Equations (A17) and (A18) were used to find the values of k_i using the optical refractive indices for the n_i. A value for k_3 may be obtained from each of two tilted-film spectra. The values of k_i obtained are shown in *Table 3*.

DISCUSSION AND FURTHER ANALYSIS OF RESULTS

The Raman and infra-red results so far given show without further analysis that the sample studied is biaxially-oriented. For a uniaxially-oriented sample the Raman intensities I_{11} and I_{22} should be equal, whereas the results in *Table 1* show clearly that they are not equal. Similarly for a uniaxial sample $I_{13} = I_{23}$ and the results show a clear difference between these two quantities. The inequality of the infra-red quantities k_1 and k_2 also suggests departure from uniaxial orientation. In order to obtain a more precise understanding of the type of orientation distribution in the sample, values of P^r_{lmn} were calculated.

For the Raman 1616 cm^{-1} line a value of –0.18 for the ratio $r = \alpha_1/\alpha_3 = \alpha_2/\alpha_3$ was taken from the work of Purvis *et al.*[5]. Using this and the six intensities I_{ii} and I_{ij}, the six simultaneous equations (18) were solved to obtain the values of the P^r_{lm0} shown in *Table 4*.

The analysis of the infra-red data to obtain values of P_{2mn} is a little more complicated because of the apparent doublet nature of each of the two absorptions. It was assumed that both members of a pair are due to the same vibrational mode of the benzene ring with the assignments given in *Figure 3*. The related investigation[18] suggests that the doublet nature arises from benzene rings in different environments, but these have not as yet been clearly identified. In order to obtain information about the distribution of orientations of all benzene rings irrespective of their environment it is necessary to average the values of ϕ_i for the two peaks, weighting them in proportion to their half-intensity widths, the values

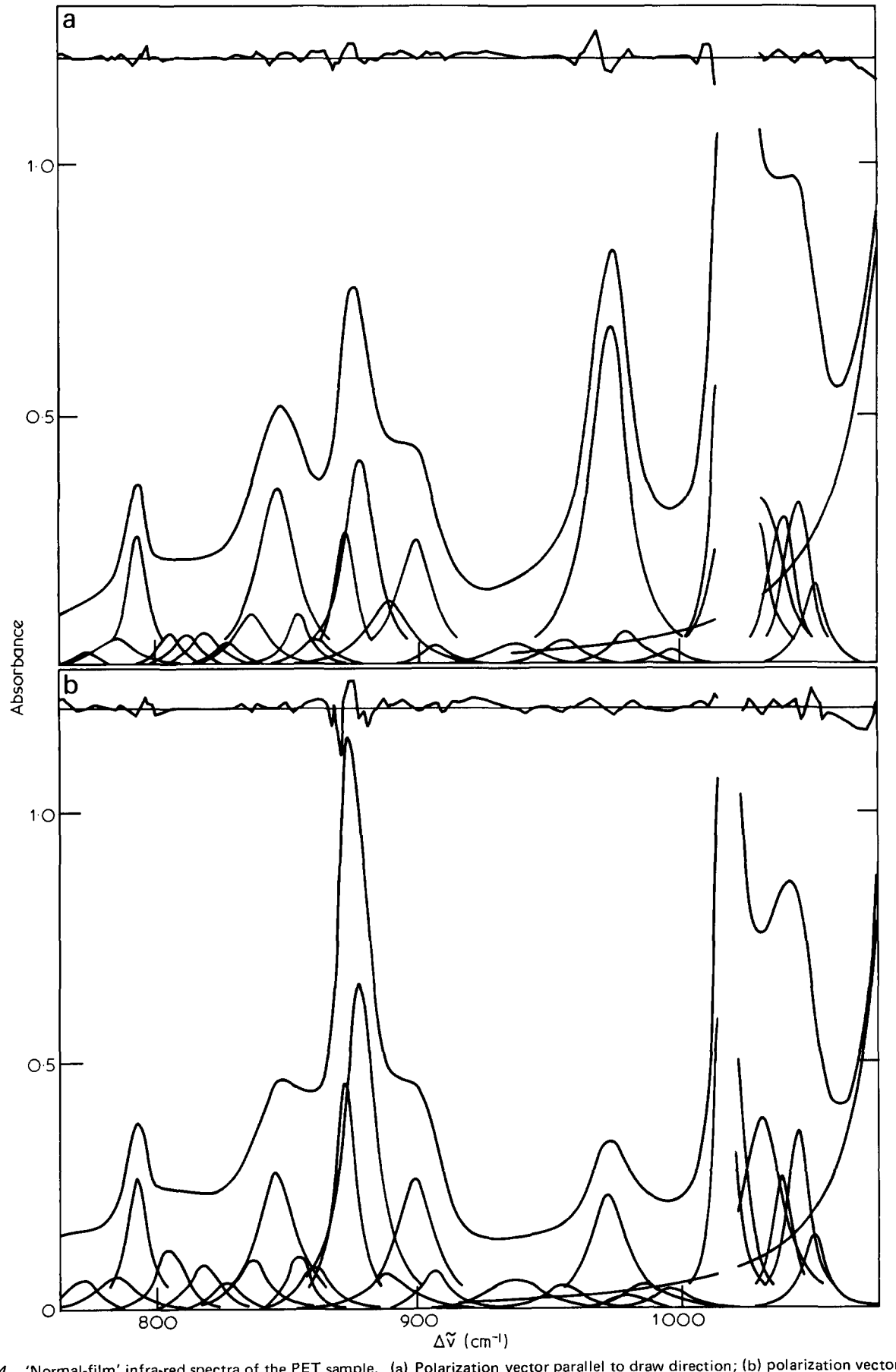

Figure 4 'Normal-film' infra-red spectra of the PET sample. (a) Polarization vector parallel to draw direction; (b) polarization vector perpendicular to draw direction. The lower curves are the fitted Lorentzian peaks (the wings of the larger peaks are omitted for clarity), the middle curve is the experimental absorbance and the upper curve represents the difference between the fitted spectrum and the observed spectrum on the same scale

of ϕ_i at the peaks having been first determined from the values of k_i and the optical refractive indices using equation (22). The values of P^r_{200} and P^r_{220} are then obtained directly from the $\bar{\phi}_i$ values for the 1017 cm^{-1} peak using equations (23) with $\theta_m = 0$ and are shown in *Table 4*. The $\bar{\phi}_i$ values for the 875 cm^{-1} peak yield values of $(P^r_{200} + 6P^r_{202})$ and $(P^r_{220} + P^r_{222})$. For the reason already given, the values of P^r_{200} and P^r_{220} obtained from the Raman data should be more accurate than those obtained from the data for the i.r. 1017 cm^{-1} peak and they have therefore been used to calculate the values of P^r_{202} and P^r_{222} shown in *Table 4*.

The results in *Table 4* show that the values of P^r_{200} and P^r_{220} obtained from the i.r. 1017 cm^{-1} absorption agree with those obtained from the Raman data, although they are appreciably less accurate than the Raman values. It is possible to see whether the values which have been obtained for the P^r_{2mn} are consistent with the measured refractive indices by making use of equations (13), provided that the appropriate P_{2mn} can be obtained from the P^r_{2mn} and that the principal values of the polarizability tensor for a monomer unit of PET are known. It is therefore necessary to consider the conformation of the monomer unit.

Two extreme conformational models have been considered. Model *A* assumes that the terephthaloyl residue is in the same conformation in the amorphous polymer as in the polymer crystal, and that the most important difference between the crystalline and non-crystalline chain is the presence of *gauche* bonds in some of the glycol residues of the amorphous chain. Model *B* assumes that there is no preferred orientation of the planes of the ester group with respect to the plane of the adjacent benzene ring in the amorphous polymer, but that the conformation of the chains is otherwise the same as in model *A*. For model *A* the mean chain direction between two *gauche* bonds coincides with what would be the crystal *c*-axis if the chain were in the crystalline region and this will be chosen as Ox^A_3; for model *B* it coincides with the C_1–C_4 direction of the benzene ring, which will be chosen as Ox^B_3.

Using the atomic coordinates determined by Daubeny *et al.*[19] and the bond polarizabilities estimated by Palmer, principal polarizabilities for model *A* were calculated by Pinnock and Ward[20]. The coordinates of the atoms of the benzene ring given by Daubeny *et al.* define a slightly distorted, non-planar benzene ring. In the present work, in order to relate the orientation of the transition moment vectors associated with the 1017 and 875 cm^{-1} infra-red peaks with that of the Raman tensor axes associated with the 1616 cm^{-1} line, the benzene ring was assumed to be planar and undistorted and to be bisected by the line C_7–C_8, C_7–C_8 which was chosen as the OX^r_3 direction. The Ox^A_1 direction was chosen to lie parallel to the plane defined by the coordinates given for C_2, C_3, C_5 and C_6. This assumption gives values of α^{eA}_1, α^{eA}_2 and α^{eA}_3, shown in *Table 5*, which differ only slightly from the corresponding values of Pinnock and Ward, and values close to these have been used in most previous work.

For model *B* the three principal symmetry axes Ox^B_3, Ox^B_1 and Ox^B_2 of the polarizability tensor for the monomer unit are along the C_1–C_4 direction, in the plane of the benzene ring and normal to the benzene ring, respectively. Since the assumption of free rotation about the ring–ester C–C bonds is made, the atoms in the monomer unit other than those of the benzene ring were imagined to rotate around the x^B_3 axis, and the average values of the projections of the bond polarizabilities onto the Ox^B_1, Ox^B_2 and Ox^B_3 axes were obtained. The principal polarizabilities obtained for model *B* are also shown in *Table 5*. These values are quite close to the values adopted by Kashiwagi *et al.* on the basis of a model in which it was assumed that the unit of structure possesses orthorhombic symmetry with the 100 plane as a plane of symmetry[1].

Table 2 I.r. absorbances

Absorption peak/cm^{-1}	A_3	A_1	A_{23}	A_{12}	Width/ cm^{-1}
873	0.28	0.47	0.88	1.05	9.54
878	0.42	0.68	0.78	0.87	13.78
1017	2.56	1.64	3.40	1.49	4.67
1020	1.49	0.48	1.60	0.93	8.04

Table 3 Values of *k*

Absorption peak/cm^{-1}	k_3	k_1	k_2 from A_{23}	k_2 from A_{12}	k_2 mean
873	0.020	0.035	0.068	0.074	0.071
878	0.030	0.049	0.047	0.041	0.044
1017	0.161	0.103	0.135	0.029	0.082
1020	0.093	0.030	0.046	0.052	0.049

Table 5 Polarizabilities of PET monomer unit

Model *A*		Model *B*	
Component	Value x 10^{23}/cm^3	Component	Value x 10^{23}/cm^3
α^{eA}_1	2.16	α^{eB}_1	1.97
α^{eA}_2	1.21	α^{eB}_2	1.37
α^{eA}_3	2.25	α^{eB}_3	2.27

Table 4 Values of P^r_{lmn}

	P^r_{200}	P^r_{220}	P^r_{202}	P^r_{222}	P^r_{400}	P^r_{420}	P^r_{440}
Raman 1616 cm^{-1} line	0.25 ±0.03	−0.013 ±0.006	–	–	0.10 ±0.05	−0.003 ±0.004	−0.007 ±0.003
Infra-red 1017 cm^{-1} absorption	0.23 ±0.05	−0.01 ±0.01	–	–	–	–	–
Infra-red 875 cm^{-1} absorption plus Raman 1616 cm^{-1} line	–	–	0.03 ±0.01	0.07 ±0.02	–	–	–

Table 6 Values of P^A_{2mn}

P^A_{200}	P^A_{220}	P^A_{202}	P^A_{222}
0.31 ±0.04	−0.021 ±0.008	0.02 ±0.01	0.07 ±0.03

For model *B*, $P^B_{2mn} = P^r_{2mn}$; for model *A* the P^A_{2mn} may be obtained from the P^r_{2mn} by using the Legendre addition theorem[12] and are shown in *Table 6*. The ratios $(2\phi^e_3 - \phi^e_2 - \phi^e_1)/(\phi^e_1 + \phi^e_2 + \phi^e_3)$ and $(\phi^e_1 - \phi^e_2)/(\phi^e_1 + \phi^e_2 + \phi^e_3)$ may now be calculated for the two models using equations (13). *Table 7* gives the results, together with the values of these ratios obtained from the measured refractive indices. It may be seen that the values obtained for both P^A_{2mn} and P^B_{2mn} are consistent with the measured refractive indices, but it is not possible to distinguish between the two conformational models on the basis of the refractive index data. The agreement of the Raman and infra-red values of P^r_{200} and P^r_{220} and the consistency of the spectroscopic data with the refractive indices suggests that the values of P^r_{lmn} obtained are reliable.

We now consider what the P^r_{2mn} tell us about the orientations of the planes of the benzene rings and about the orientations of the polymer chain axes. For this purpose, it is useful to write the average values of the squares of the direction cosines of the axes Ox^r_i with respect to the $OX_1X_2X_3$ system, $\cos(x^r_i X_j)$, in terms of the P^r_{2mn}, i.e.:

$$\langle\cos^2(x^r_1X_1)\rangle = \frac{1}{3} + \frac{1}{6}P^r_{200} - P^r_{220} - P^r_{202} + P^r_{222} \quad (25a)$$

$$\langle\cos^2(x^r_1X_2)\rangle = \frac{1}{3} + \frac{1}{6}P^r_{200} + P^r_{220} - P^r_{202} - P^r_{222} \quad (25b)$$

$$\langle\cos^2(x^r_1X_3)\rangle = \frac{1}{3} - \frac{1}{3}P^r_{200} + 2P^r_{202} \quad (25c)$$

$$\langle\cos^2(x^r_2X_1)\rangle = \frac{1}{3} + \frac{1}{6}P^r_{200} - P^r_{220} + P^r_{202} - P^r_{222} \quad (25d)$$

$$\langle\cos^2(x^r_2X_2)\rangle = \frac{1}{3} + \frac{1}{6}P^r_{200} + P^r_{220} + P^r_{202} + P^r_{222} \quad (25e)$$

$$\langle\cos^2(x^r_2X_3)\rangle = \frac{1}{3} - \frac{1}{3}P^r_{200} - 2P^r_{202} \quad (25f)$$

$$\langle\cos^2(x^r_3X_1)\rangle = \frac{1}{3} - \frac{1}{3}P^r_{200} + 2P^r_{220} \quad (25g)$$

$$\langle\cos^2(x^r_3X_2)\rangle = \frac{1}{3} - \frac{1}{3}P^r_{200} - 2P^r_{220} \quad (25h)$$

$$\langle\cos^2(x^r_3X_3)\rangle = \frac{1}{3} + \frac{2}{3}P^r_{200} \quad (25i)$$

The values of the averages for the PET film studied are shown in *Table 8* and the uncertainty on each of the values is ±0.02. For a randomly-oriented sample all the averages would have the value 1/3.

The values of $\langle\cos^2(x^r_3X_i)\rangle$ for i = 1,2 and 3 provide information about the preferential orientation of the C_1–C_4 direction with respect to the sample axes. The fact that $\langle\cos^2(x^r_3X_3)\rangle$ is the largest of the three means that the C_1–C_4 axes are preferentially oriented towards the draw direction. Of the remaining two averages, $\langle\cos^2(x^r_3X_2)\rangle$ is greater than $\langle\cos^2(x^r_3X_1)\rangle$, and this indicates that within the overall preferential orientation towards the draw direction there is some preferential orientation normal to the plane of the fi film. This may be reinterpreted to mean that those benzene rings whose C_1–C_4 axes lie closer to the plane of the sheet, OX_1X_3, than to the OX_2X_3 plane have these axes more highly oriented towards the draw direction, on average. Referring to equations (25g) and (25h) this information is seen to be directly given by the sign of P^r_{220}, i.e. $\langle\cos^2(x^r_3X_1)\rangle$ is greater than or less than $\langle\cos^2(x^r_3X_2)\rangle$ according to whether the sign of P^r_{220} is positive or negative. Uniaxial orientation of the C_1–C_4 axes about the draw direction is indicated if P^r_{220} is zero.

An idea of the extent of biaxial orientation of the C_1–C_4 axes is obtained if the limits on the range of values that P^r_{220} may take are known. Referring to equation (6a), $(1 - \cos^2\theta$ is always positive, and therefore the upper and lower limits on P_{220} are obtained by putting ϕ equal to 0 and $\pi/2$, respectively. Expressing $(1 - \cos^2\theta)$ in terms of P_{200} gives:

$$|P_{220}| < \frac{1}{6}(1 - P_{200}) \quad (26)$$

Thus, for the value of P_{200} found here, $|P^r_{220}|$ must be less than 0.125. The fact that the observed value for $|P^r_{220}|$ is small compared with 0.125 means that there is only a

Table 7 Comparison of data from spectroscopic measurements with those from refractive indices

Quantity	Calculated from spectroscopic data: Model *A*	Calculated from spectroscopic data: Model *B*	Calculated from refractive indices
$\frac{2\phi^e_3 - \phi^e_1 - \phi^e_2}{\phi^e_1 + \phi^e_2 + \phi^e_3}$	0.08 ±0.02	0.07 ±0.02	0.080 ±0.001
$\frac{\phi^e_1 - \phi^e_2}{\phi^e_1 + \phi^e_2 + \phi^e_3}$	0.02 ±0.01	0.01 ±0.01	0.013 ±0.001

Table 8 Values of $\langle\cos^2(x^r_iX_j)\rangle$ and $\langle\cos^2(x^A_iX_j)\rangle$

	X_1	X_2	X_3
x^r_1	0.43	0.27	0.30
x^r_1	0.35	0.45	0.20
x^r_3	0.22	0.28	0.50
x^A_1	0.46	0.27	0.27
x^A_2	0.35	0.46	0.19
x^A_3	0.19	0.27	0.54

small tendency for the C_1–C_4 axes to be preferentially oriented towards the normal to the plane of the film.

The values of $\langle\cos^2(x_2^r X_i)\rangle$ for $i = 1$, 2 and 3 provide information about the preferential orientation of the plane of the benzene ring. Interpreting the results in a manner similar to that used for the $\langle\cos^2(x_3^r X_i)\rangle$, it may be seen that the planes of the benzene rings are preferentially oriented towards the plane of the sheet. This 'planar orientation' of the benzene rings has been detected in the crystalline regions of other one-way drawn sheets of PET using X-ray diffraction methods[21,22]. The degree of 'planar orientation' is seen to be comparable with the degree of orientation of the C_1–C_4 axes towards the draw direction.

If the conformational model *B* is assumed, the distribution of orientations of the chain axes is the same as that of the C_1–C_4 axes. If the conformational model *A* is assumed, information about the preferred orientation of the chains may be obtained by calculating the $\langle\cos^2(x_i^A X_j)\rangle$. These averages have the same form as equations (25a–i) with x_i^r replaced by x_i^A and the P_{2mn}^r replaced by the P_{2mn}^A. The values are given in *Table 8*. Once again the uncertainty in these results is ±0.02. We see that for model *A* both the orientation of the chain axes towards the draw direction and the extent of the biaxial orientation of the chain axes are slightly greater than for model *B*.

For either model, however, the results indicate that the chain axes are more highly oriented towards the draw direction the closer they lie to the plane of the sheet. This is contrary to the prediction of any of the simple models used to explain the production of orientation during the deformation process, such as the rubber[23] or pseudo-affine[24] models. These models predict that the chain axes in a one-way drawn material should be less highly oriented the closer they lie to the plane of the sheet. The models, however, assume no preferred orientation around the chain axes, and this assumption does not hold for the present one-way drawn sheet, so that a direct comparison cannot be made. One possible explanation of the result is that, on drawing, the benzene rings begin to orient into the plane of the sheet and this makes it easier for chains near this plane to slip past each other and become more highly aligned with the draw direction. Thus for low draw the chains near the plane of the sheet will tend to be more highly oriented towards the draw direction, as is the case for the PET film studied here. On further drawing the effect of holding the film at constant width might be expected to slow down this process of slipping, and the chains would then orient into the plane of the sheet, i.e. P_{220}^A or P_{220}^B would change sign. Studies in progress on more highly oriented sheets show that this change of sign does indeed take place.

We now consider briefly the significance of the values of P_{400}^r, P_{420}^r and P_{440}^r obtained from the Raman results. By considering the forms of the functions of θ which appear in equations (5c), (6b) and (6c), it may be shown that the absolute limits of these three types of orientation parameter are given by:

$$-\frac{3}{7}(= 0.429) \leqslant P_{400} \leqslant 1 \qquad (27a)$$

$$|P_{420}| \leqslant 3/56\ (= 0.0536) \qquad (27b)$$

$$|P_{440}| \leqslant 1/16\ (= 0.0625) \qquad (27c)$$

The observed values of P_{400}^r, P_{420}^r and P_{440}^r, viz. 0.1, −0.003 and −0.007, respectively, lie well inside these limits. It may be shown, however, that the limits on the values of the members of any set of P_{lmn} are not independent, because the distribution function, $N(\theta, \phi, \psi)$ must be positive for all (θ, ϕ, ψ). In general the values of q for different P_{lmn} are compatible only if the point corresponding to them lies within a restricted 'volume' in a q-dimensional space each of whose axes represents values of one of the P_{lmn}. This volume lies within, but is only a part of, the volume defined by the set of absolute limits on the P_{lmn}.

The point corresponding to the present set of seven experimentally-determined values of P_{lmn}^r may be shown to lie well within the restricted 'volume' in the appropriate seven-dimensional space, and this indicates that the distribution of orientations is well away from the rather special types of distribution to which points on the boundary of the allowed 'volume' correspond. Since $(1 - 2\cos^2\theta + \cos^4\theta)$ is positive for all θ, equation (6c) shows that the observed negative value of P_{440}^r indicates a tendency for the projections of the C_1–C_4 directions on the OX_1X_2 plane to lie near ±45° to OX_1 or OX_2 rather than near to either OX_1 or OX_2. Thus the tendency, already deduced from the value of P_{220}^r, for the C_1–C_4 directions to lie nearer to the OX_2X_3 plane than to the OX_1X_3 plane probably corresponds to a fairly broad distribution. This is consistent with the suggestion already given that the latter tendency may arise from the greater ease with which those chains that lie nearer to the OX_1X_3 plane become preferentially oriented towards the draw direction once preferential orientation of the rings has taken place. Further discussion of the values of P_{400}^r, P_{420}^r and P_{440}^r and of their significance in understanding the mechanical properties of biaxially-oriented samples will be deferred to a subsequent paper, which will deal with the results of measurements on the more highly oriented sheets already referred to.

CONCLUSIONS

Raman and infra-red spectroscopies have been applied to the study of molecular orientation in 3.5:1 'one-way' drawn PET film. The results obtained from the two techniques agree well and the measured values of the three principal refractive indices also fit into the overall picture of molecular orientation obtained. The results indicate that there is planar orientation of the benzene rings and that at the rather low degree of overall orientation obtained at this draw ratio the chain axes are preferentially oriented away from the plane of the film. The latter result is contrary to expectation, but the degree of this preferential orientation is quite small.

ACKNOWLEDGEMENTS

We are indebted to Imperial Chemical Industries, Plastics Division, Welwyn Garden City, for providing the materials and as the industrial sponsor of the Science Research Council CASE studentship held by I. J. Hutchinson during the course of this work. We especially wish to thank Dr. H. A. Willis and Mrs. V. I. Zichy for their continued interest and encouragement. In particular, we are grateful to Mrs Zichy for stimulating our interest in the tilted-film infra-red spectroscopic measurements, and giving advice on the experimental procedures involved.

We should like to thank the SRC for providing a research grant for spectroscopic studies of oriented polymers.

REFERENCES

1 Kashiwagi, M., Cunningham, A., Manuel, A. J. and Ward, I. M. *Polymer* 1973, **14**, 111
2 Kashiwagi, M., Folkes, M. J. and Ward, I. M. *Polymer* 1971, **12**, 697
3 Nishijima, Y. *J. Polym. Sci. (C)* 1970, **31**, 353
4 Nobbs, J. H., Bower, D. I. and Ward, I. M. *Polymer* 1976, **17**, 25
5 Purvis, J., Bower, D. I. and Ward, I. M. *Polymer* 1973, **14**, 398
6 Purvis, J. and Bower, D. I. *Polymer* 1974, **15**, 645
7 Purvis, J. and Bower, D. I. *J. Polym. Sci. (Polym. Phys. Edn)* 1976, **14**, 1461
8 Cunningham, A., Ward, I. M., Willis, H. A. and Zichy, V. *Polymer* 1974, **15**, 749
9 Roe, R-J. *J. Appl. Phys.* 1965, **36**, 2024
10 Nomura, S., Kawai, H., Kimura, I. and Kagiyama, M. *J. Polym. Sci. (A-2)* 1970, **8**, 383
11 Cunningham, A., Davies, G. R. and Ward, I. M. *Polymer* 1974, **15**, 743
12 Bower, D. I. *J. Polym. Sci. (Polym. Phys. Edn)*, 1972, **10**, 2135
13 Bower, D. I. *J. Phys. (B)* 1976, **9**, 3275
14 Varsanyi, G., 'Vibrational Spectra of Benzene Derivatives', Academic Press, New York, 1969, p 152
15 Julien-Laferriere, S. and Lebas, J-M. *Spectrochim. Acta* 1971, **27A**, 1337
16 Grime, D. and Ward, I. M. *Trans. Faraday Soc.* 1958, **54**, 959
17 Boerio, F. J., Bahl, S. K. and McGraw, G. E. *J. Polym. Sci. (Polym. Phys. Edn)* 1976, **14**, 1029
18 Hutchinson, I. J., Ward, I. M., Willis, A. and Zichy, V. *Polymer* 1980, **21**, 55
19 Daubeny, R. de P., Bunn, C. W. and Brown, C. J. *Proc. Roy. Soc., London (A)* 1954, **226**, 531
20 Pinnock, P. R. and Ward, I. M. *Br. J. Appl. Phys.* 1964, **15**, 1559
21 Brown, N., Duckett, R. A. and Ward, I. M. *Phil. Mag.* 1968, **18**, 483
22 Heffelfinger, C. J. and Burton, R. C. *J. Polym. Sci.* 1960, **47**, 289
23 Treloar, L. R. G. 'The Physics of Rubber Elasticity', 3rd Edn, Oxford, 1975, Ch 4, 6
24 Ward, I. M. 'Mechanical Properties of Solid Polymers', Wiley, London, 1971, p 258

APPENDIX

Determination of infra-red absorbances and refractive indices from normal and tilted-film measurements

Consider a parallel-sided film either sandwiched between two parallel-sided plates of a material of refractive index n_0 and placed in the i.r. spectrometer so that the film is normal to the incident infra-red beam or sandwiched between two prisms of the material and placed so that the beam traverses a parallel-sided block within which the film is held so that it is inclined at angle θ_i, to the beam. Let I_T be the observed transmitted intensity at angular frequency ω within an isolated absorption peak and I'_T that in the background close to the peak but sufficiently far away that the effect of the absorption is negligible. Then it is easy to show[11] that:

$$\frac{I'_T}{I_T} = \frac{(1-R')^2}{(1-R)^2}\frac{1}{L} \tag{A1}$$

where L is the attenuation within the sample at the frequency ω and R and R' are the fractions of the incident intensity reflected at each interface between the film and the medium on either side of it at the frequency ω and in the background, respectively. (No account is taken of possible multiple reflections in the plates for the normal incidence assembly). Thus the apparent absorbance A is given by:

$$A = \log_{10}\frac{I'_T}{I_T} = 0.4343\,(-\ln L + \ln T) \tag{A2}$$

where

$$T = \left(\frac{1-R'}{1-R}\right)^2 \tag{A3}$$

We consider first the true absorption term, using a generalization of a treatment given by Born and Wolf ('Optics', Pergamon Press, 5th Edn, 1975, p 615) for the refraction of a plane wave at the interface between a non-absorbing and an absorbing medium. In the complex notation, the amplitude of a plane wave is written $e^{i\hat{\delta}}$, where $\hat{\delta} = \delta' - i\delta''$ so that $e^{i\delta} = e^{\delta''}e^{i\delta'}$. Thus $e^{\delta''}$ represents the real amplitude and δ' represents the real phase angle. In an absorbing medium both δ' and δ'' are functions of position. If the wave is a simple homogeneous plane wave then δ' and δ'' have the same dependence on position and $\hat{\delta}$ can be written $\hat{\delta} = \hat{k}\mathbf{r}\cdot\mathbf{s}$ where $\mathbf{r}$ is the position vector, $\mathbf{s}$ is the real unit vector whose direction is that of the normal to the planes of constant $\hat{\delta}$, (i.e. constant δ' and δ'') and $\hat{k}$ is a complex scalar, so that $\hat{k}s$ represents a complex wavevector. If s measures displacement in the direction of $\mathbf{s}$, then the complex phase of the wave is $\hat{\delta} = \hat{k}s$. In general, however, the planes of constant real phase, i.e. constant δ' do not coincide with the planes of constant real amplitude, i.e. planes of constant δ''. This is clearly so for the refracted wave incident at an angle to the surface of even an isotropic absorbing medium, where the planes of constant real phase in the medium will not be parallel to the surface but the planes of constant amplitude must be, as consideration of continuity at the boundary shows. In general, therefore, the unit vector $\mathbf{s}$ must also be regarded as complex and it will be written $\hat{\mathbf{s}}$. If $\hat{n}$ is the complex refractive index the complex speed of light in the medium is $\hat{v} = c/\hat{n}$ and the complex magnitude of the wavevector is:

$$\hat{k} = \omega/\hat{v} = \omega\hat{n}/c \tag{A4}$$

We define the real and imaginary parts of the principal refractive indices by:

$$\hat{n}_i = n_i(1 - i\kappa_i) = n_i - ik_i \tag{A5}$$

The k in this equation should not be confused with $\hat{k}$, the complex magnitude of the wavevector.

Consider a plane wave incident at angle θ_i on the plane face of a biaxially-oriented film of absorbing medium and choose axes $Oxyz$ so that Oz is normal to the plane of the film and Ox and Oy coincide with the other two principal axes of the film. If the electric vector lies in the plane of incidence and if this is also the Oxz plane, we can write Snell's Law in the complex form:

$$\hat{s}_x = \sin\hat{\theta}_t = (n_0/\hat{n})\sin\theta_i$$

$$\hat{s}_y = 0 \tag{A6}$$

$$\hat{s}_z = \cos\theta_t$$

where $\hat{\theta}_t$ may be regarded as a complex angle of refraction. It may be shown (Born and Wolf, *Ibid.* p 708) that the following general equation (Fresnel's equation) applies to any plane wave in the medium:

$$\frac{\hat{s}_x^2}{\hat{v}^2 - \hat{v}_x^2} + \frac{\hat{s}_y^2}{\hat{v}^2 - \hat{v}_y^2} + \frac{\hat{s}_z^2}{\hat{v}^2 - \hat{v}_z^2} = 0 \quad \text{(A7)}$$

where

$$\hat{v}_x = c/\hat{n}_x,\ \hat{v}_y = c/\hat{n}_y,\ \hat{v}_z = c/\hat{n}_z \quad \text{(A8)}$$

Using equation (A6), equation (A7) may be written:

$$\hat{v}^2 = \hat{v}_z^2\hat{s}_x^2 + \hat{v}_x^2\hat{s}_z^2 \quad \text{(A9)}$$

It then follows from equations (A6) and (A9) that

$$\hat{s}_x/\hat{v} = (n_0 \sin\theta_i)/c \quad \text{(A10)}$$

and that

$$\hat{s}_z/\hat{v} = (an_x/c)(\cos b - \kappa_x \sin b) + i(an_x/c)(\kappa_x \cos b + \sin b) \quad \text{(A11)}$$

where

$$a^2\cos 2b = 1 - \frac{n_0^2}{n_z^2}\,\frac{1-\kappa_z^2}{(1+\kappa_z^2)^2}\sin^2\theta_i \quad \text{(A12a)}$$

$$a^2\sin 2b = \frac{n_0^2}{n_z^2}\,\frac{2\kappa_z}{(1+\kappa_z^2)^2}\sin^2\theta_i \quad \text{(A12b)}$$

Since

$$\hat{\delta} = \hat{k}(\mathbf{r}\cdot\hat{\mathbf{s}}) = \omega\left(\mathbf{r}\cdot\frac{\hat{\mathbf{s}}}{\hat{v}}\right) = \omega\left(x\frac{\hat{s}_x}{\hat{v}} + z\frac{\hat{s}_z}{\hat{v}}\right) \quad \text{(A13)}$$

we have

$$\hat{\delta} = \frac{\omega}{c}\,[xn_0\sin\theta_i + z\,an_x(\cos b - \kappa_x \sin b) + iza\,n_x(\kappa_x\cos b + \sin b)] \quad \text{(A14)}$$

Thus the amplitude of the wave decays as:

$$\exp[-(\omega/c)an_x(\kappa_x\cos b + \sin b)z] \quad \text{(A15)}$$

and

$$-\ln L = 2(\omega/c)an_x(\kappa_x\cos b + \sin b)t = 4\pi t\tilde{\nu}an_x(\kappa_x\cos b + \sin b) \quad \text{(A16)}$$

where $\tilde{\nu}(= 1/\lambda = \omega/2\pi c)$ is the wavenumber.

If $\theta \to 0$ then $a \to 1$ and $b \to 0$ and:

$$-\ln L \to 4\pi t\tilde{\nu}n_x\kappa_x = 4\pi t\tilde{\nu}k_x \quad \text{(A17)}$$

It is easy to show that for the electric vector perpendicular to the plane of incidence (Oxz), i.e. parallel to Oy, the expressions for $-\ln L$ are obtained from the equations above simply by substituting n_y for n_x and n_z and substituting κ_y for κ_x and κ_z. If $t = 30\ \mu m$ and $\nu = 1000\ cm^{-1}$, which are typical values, and $k = 0.1$ are substituted into equation (A17) the absorbance $A = -0.4343 \ln L$ is found to be 1.64 which corresponds to a transmission of only 2.3%. This is at, or lower than, the limit which can be reliably determined using a conventional infra-red spectrophotometer. We thus take $k = 0.1$ to be the largest value we need to consider.

The right hand side of equation (A16) may be expanded in odd powers of κ_i; if only the first term is kept then:

$$-\ln L = 4\pi t\tilde{\nu}\left(\frac{n_x}{n_z}\right)\frac{n_z^2\kappa_x + n_0^2\sin^2\theta_i(\kappa_z - \kappa_x)}{\sqrt{n_z^2 - n_0^2\sin^2\theta_i}} \quad \text{(A18)}$$

For an isotropic sample neglect of terms in κ^3 and higher powers produces an error of only 0.3% in $-\ln L$ for $k = 0.1$, with $n_0 = 1.5$, $n = 1.6$, which are typical values, so that equation (A18) should be a good approximation. Equations (A16) or (A18), and equation (A17), together with their equivalents for Oyz as the plane of incidence constitute a set of six equations in the six quantities n_i, κ_i, or n_i, k_i which could thus be determined, from a suitable set of measurements, for any point in the spectrum.

The quantities required for the evaluation of the orientation parameters are the ϕ_i given by equation (22), viz.:

$$\phi_i = \frac{4\pi}{3}\alpha'' = \frac{6n_ik_i}{(n_i^2+2)^2 + (2n_i^2 - 4)k_i^2 + k_i^4} \quad \text{(A19)}$$

For $n = 1.6$ and $k = 0.1$, neglect of the terms in k^2 and k^4 changes the expression on the right hand side of equation (A19) by only 0.05% so that to a very good approximation:

$$\phi_i = \frac{4\pi}{3}\alpha'' = \frac{6n_ik_i}{(n_i^2+2)^2} \quad \text{(A20)}$$

We assume that for an absorption of non-zero width the required measure of ϕ_i is its mean value over the absorption peak. Thus in principle it is necessary to know the values of n_i and k_i at all frequencies. Fortunately, however, both a simple theoretical model and experimental evidence show that the absorbance spectrum of a single isolated infra-red absorption is of Lorentzian line-shape to a very good approximation.

If we assume that the contribution α_m of a single vibrational mode of angular frequency ω_m to the complex polarizability of the material is given by:

$$\alpha_m = \frac{a_m}{(\omega_m^2 - \omega^2) + i\gamma_m\omega} \quad \text{(A21)}$$

where α_m is a constant proportional to the concentration of absorbers and γ_m is a damping constant, it is easy to show that the imaginary part, α_m'', of α_m approaches a Lorentzian as the linewidth becomes smaller. For a line of half-intensity width 10 cm^{-1} at 1000 cm^{-1} the lineshape differs from a Lorentzian by only ~0.2% or less of the peak height at any frequency. It may also be shown from the equation for the real part of α_m, derivable from equation (A21), that n varies with ω by only about 2.5% within such a narrow peak. From this it follows that the lineshape corresponding to equation (A17) differs from a Lorentzian by only 1.3% of the peak height at any frequency. Experimental evidence on isolated infra-red absorption peaks confirms that they generally approach closely to the Lorentzian line shape (Baker *et al. Spectrochim. Acta (A)* 1978, **34**, 683).

The first and second terms in equation (A18) may

similarly be shown to deviate from Lorentzians by only about 0.5 and 3%, respectively, for $\theta_i = 45^\circ$, so that it should be a good approximation to analyse the directly observed absorbance spectrum as the sum of a set of overlapping Lorentzians and to assume that the peak heights are related to n_i and k_i by equations (A17) and (A18), where k_i is now the contribution of the absorbance under consideration to the total k_i. Quantities proportional to ϕ_i may then be calculated from equation (A20).

Finally we consider the reflection term in the apparent absorbance and for simplicity restrict attention to a single absorption of an isotropic medium. We assume that n_0 does not vary significantly with frequency, that $k = 0$ outside the absorption peak, and that we can neglect the small variation of n caused by a single absorption peak, so that it has the same value within and outside the peak. It then follows from Fresnel's equations for the reflection coefficients written in the complex form (Born and Wolf, *Ibid.* p 617) that for normal incidence, for incidence at 45° with the electric vector in the plane of incidence and for incidence at 45° with the electric vector perpendicular to the plane of incidence, the apparent absorbances A_R due to reflection are approximately 0.06, 0.002 and 0.15%, respectively, of the true absorbance. This shows that the reflection correction is completely negligible and we may therefore reduce equation (A2) to

$$A = -0.4343 \ln L \qquad \text{(A22)}$$